Evolutionary developmental biology of bitterling fish

Yi, W.

Chapter 5 Pre-hatching early embryonic development in the rosy bitterling (*Rhodeus ocellatus*)

Wenjing Yi[1], Martin Reichard[2], Martin Rücklin[3], and Michael K. Richardson[1]

1, Institute of Biology, University of Leiden, Sylvius Laboratory, Sylviusweg 72, 2333BE, Leiden, the Netherlands.

2, Institute of Vertebrate Biology, Czech Academy of Sciences, Kvetna 8, 603 65 Brno, Czech Republic.

3, Vertebrate Evolution, Development and Ecology, Naturalis Biodiversity Center, Postbus 9517, 2300 RA Leiden, The Netherlands

Manuscript in preparation

Abstract

Bitterlings are Cynipid fish of the subfamily Acheilognathinae. All bitterlings have a brood-parasitic early life history, in which embryos parasitise the internal gill space of fresh-water unionid mussels (Unionide). Our aim in this study is to examine early stages of development in this species in detail because they are otherwise known only from a few descriptive studies. We hypothesise that early development in the bitterling will show modifications related to brood parasitism. We have examined the expression of the genes *fgf8a*, *krt8*, *msx3* and *ctslb* by whole-mount *in situ* hybridization (WISH) in early pre-hatching development and hatching of the rosy bitterling (*Rhodeus ocellatus*). We find that a unique aspect of bitterlings among teleosts is their modified pattern of convergent-extension movements during gastrulation and neurulation. This leads to the rostro-caudal inversion of the embryo in the chorion, a phenomenon refered as blastokinesis. Further, we suggest that blastokinesis in the rosy bitterling is functional because it provides optimal positioning of the post-hatching embryo in the gill space of the host mussel. More generally, our study provides an example of variation in yolk shape and egg size consistent with the concept of developmental penetrance of adaptations on later stages.

Introduction

The rosy bitterling (*Rhodeus ocellatus*, Kner, 1866) is a teleost fish of the carp and minnow family (Cyprinidae). Together with approximately 70 other species of bitterling, it belongs to the subfamily Acheilognathinae (Cheng et al., 2014; Kawamura et al., 2014). All Acheilognathinae have a brood parasitic life history, and development is similar in the entire group (Smith et al., 2004). During the mating season (April to June) female bitterlings develop long ovipositors, that they use to deposit their eggs into the gills of a living mussel through its exhalant siphon (Awata et al., 2019; Chang, 1948; Chang and Wu, 1947; Khlopova and Kul'bachnyi, 2013; Olt, 1893; Smith et al., 2014).

After deposition of the eggs by the female into the mussel, the male releases sperm into the inhalant siphon of the mussel. The incoming water current then transfers the spermatozoa through the gills, where it fertilizes the eggs. Once the eggs are hatched, the larvae reside inside the mussel. There, the larvae compete with their host for oxygen (Spence and Smith, 2013). After approximately one month, the larvae are able to free themselves from the interlamellar space, migrate to the exhalant cavity at the gill base and leave their host (Aldridge, 1999; Chang, 1948; Leung, 2014; Smith, 2016; Suzuki, 2006).

An important question in bitterling evo devo is: from what stage of development does rosy bitterling show adaptations to the brood parasitic life-style? In addressing this question, we note already some derived conditions at the earliest stages post-laying. The fresh eggs of rosy bitterling eggs have a characteristic morphology. Unlike most teleost eggs, which are approximately spherical (Kunz, 2004), the rosy bitterling spawns long, spindle-shaped eggs. The eggs are also relatively large compared to other carp species (Aldridge, 1999; Kim and Park, 1985). The fertilized egg has a characteristic shape like a balloon, with an enlarged, spherical vegetal hemisphere and a small, tubular animal hemisphere (Chang, 1948). Another bitterling specialization is the shape of the yolk sac. Its anterior portion expands into a pair of widened yolk sac extensions (YSEs) immediately after hatching, eventually giving the whole embryo the shape of an arrowhead (Arai, 1988; Nagata and Miyabe, 1978; Virta and Cooper, 2009b).

Chang and Wu (1947) described in detail a phenomenon: the rostro-caudal inversion of the embryo in the chorion which they called 'blastokinesis'. The blastokinesis is autonomous, in the sense that it is not subject to external forces such as gravity or the internal pressure of the chorion (Chang and Wu, 1947). According to Chang and Wu (1947), the whole process of blastokinesis takes place over 5.5 hours (at 27-29 °C). It begins at a stage just before the closure of the blastopore, and ends at the initial phase of YSEs formation when there are 10-12 somite pairs. Then, the embryos begin to hatch. Those authors also noticed that, after the closure of the blastopore, the embryo grows conspicuously in length and blastokinesis takes place more slowly than in the first 2.5 h.

The rosy bitterling (*R. ocellatus*) is the only teleost species that has been to show blastokinesis during early development. Blastokinesis proper is more familiar to researchers of insect development (Panfilio, 2008; Panfilio, 2009). As suggested by Needham (1942), blastokinesis in insects may agitate the yolk material, facilitating the supply of yolk nutrients to the embryo. At present, it is not clear whether blastokinesis in these two taxa are homologous or convergent evolution, and this uncertainty provides additional motivation for further research on blastokinesis in the bitterling.

In Chapter 2 we hypothesized that blastokinesis was caused by the processes of gastrulation, neurulation and somitogenesis. Therefore, we named stages before the closure of blastopore as convergence, extension and migration, and indexed later stages by somite number. Here, we have studied the expression of highly conserved marker genes by whole-mount *in situ* hybridization (WISH) to visualize the early pre-hatching development of *R. ocellatus* and test that hypothesis. Convergent extension (CE) is a collective cell movement, a highly conserved developmental process in all metazoans (Tada and Heisenberg, 2012). CE results in the narrowing and lengthening of an embryonic field along a defined axis (Williams and Solnica-Krezel, 2020). FGF signaling, including *fgf8a*, has an essential role in the coordination of cell movements during gastrulation and neurulation (Dorey and Amaya, 2010). The neural plate undergoes CE movements, which result in lengthening and narrowing of the neural plate along the anterior-posterior and medial-lateral axes. Convergence of the neural plate can be identified by the specific expression domain of the gene *msx3* (Phillips et al., 2006).

We have also use time-lapse photography, histology and microCT methods to analyze the early development of bitterling, to explore the phenomenon of blastokinesis and its possible adaptive significance. To examine the cellular composition of the YSEs we studied the expression of the genes *krt8* and *ctslb*. The gene *krt8* is an epidermal marker for keratinocyte differentiation (Eisenhoffer et al., 2017; Imboden et al., 1997). The expression of *ctslb* is a reliable marker for the hatching gland cells (Vogel and Gerster, 1997).

Materials and Methods

Rhodeus ocellatus embryos

Rhodeus ocellatus embryos of synchronized developmental age were provided by the Reichard lab of the Institute of Vertebrate Biology in Brno, Czech Republic by IVF (*in vitro* fertilization). After fixation of the embryos of various developmental stages in 4%PFA, they were dehydrated step-wise in methanol and stored in 100% methanol (MeOH) at -20°C. The developmental staging of the embryos was based on Nagata and Miyabe (Nagata & Miyabe, 1978) and on the staging table from the Chapter 2 of this thesis. Two or three replicates were used for each stage.

Danio rerio embryos

Embryos of the zebrafish *Danio rerio* (AB/TL line) were collected in the fish facility of the Institute of Biology Leiden. The eggs were fertilized by 1:1 spawning (single crossing) at the beginning of the light period (14 h light, 10 h dark). The fertilized eggs were collected and incubated in egg water (containing 60 µg/ml “Instant Ocean” sea salts) at 28.5 °C. After collection, the embryos were immediately fixated in 4% paraformaldehyde (pFA). Fixed embryos were dehydrated step-wise in MeOH and stored in 100% MeOH at -20 °C. The developmental stages were determined according to Kimmel *et al*. (Kimmel et al., 1995). For each stage, ten replicates were used.

Whole-mount *in situ* hybridization

Whole-mount *in situ* hybridization (WISH) was performed according to the protocol of Thisse *et al*., (2004).

MicroCT

The following protocol is based on Metscher (2009), and Babaei, Hong et al. (2016). The fixative was 3% pFA and 1% glutaraldehyde in 0.1mol l^{-1} phosphate buffered saline (PBS), pH 7.0 at 4 °C overnight. After rinsing in PBS (2 x 10 min), specimens were stained with iodine-potassium iodide (1% iodine in 2% potassium iodide) for 12 h or phosphotungstic acid (0.3% phosphotungstic acid in 70% ethanol) for ≥ 24 h. Staining was carried out on a rotary mixer at 6 revolutions per minute. After staining, the embryos were stored at 4 °C in 70% ethanol. Samples were immobilized in 1% low melting-point agarose, sealed with paraffin oil and parafilm, and stabilized in a polystyrene tube during scanning.

The raw data for 3-D imaging of the samples were acquired using an Xradia 520 Versa 3-D X-ray microscope (Zeiss). The X-ray source was set to 80/7 or 40/3 (keV/W). A thin LE1 filter was used to avoid beam hardening artifacts. To obtain high resolution images, a CCD (charge-coupled device) optical objective (4x) was used. The isotropic voxel size for overview scanning of the whole embryo was 2-3 µm. For detailed scanning of the head region, the isotropic voxel size was set to < 1.5 µm. Each sample was rotated 180+fan degrees along the anterior-posterior (AP) axis. The projection images acquired were checked for sample drifting then reconstructed if of acceptable quality.

3D-reconstrutions and annotation

Virtual sections were created from the microCT data and were assembled with Avizo software (Avizo 9.5, Thermo Scientific™) using volume rendering for 3D visualization.

Results

Convergence- extension is the first phase of blastokinesis

From the onset of gastrulation, *fgf8a* early expression is in the marginal cells around the entire periphery of the blastoderm (Fig. 1A). At the mid-gastrula stage, a dorsoventral gradient expression appears in the marginal region (Fig. 1B), marking the establishment of the dorsoventral axis of the embryo. At this stage, the strongest expression of *fgf8a* is in the embryonic shield, the teleost equivalent of Spemann's organizer (Fürthauer et al., 1997), located at the dorsal midline (Fig. 1C). Along the dorsal midline, towards the animal pole, two transverse bands of weak hybridization are recognizable as the bilateral hindbrain primordia (Fig. 1C and D).

According to Chang and Wu (1947), at the beginning of blastokinesis, the embryo starts to migrate on the yolk ball gradually, the head passing the animal pole and migrating to the opposite side; the whole embryo thereby becomes hook-shaped. The blastopore has not yet closed (Fig. 2A, and on this basis, the embryo is at an equivalent stage as that depicted in Fig. 1D in Chang and Wu (1947).

The expression of *fgf8a* at this stage marks the progress of gastrulation. Its dorsoventral expression gradient persists up to the closure of blastopore, when it surrounds the yolk plug (Figure 2A). We have noted (in Chapter 2) that the yolk plug of the bitterling embryo is located not at the vegetal pole but dorsal to it, a position resulting from the asymmetry of convergence and extension movements between the dorsal and ventral blastoderm during gastrulation. The zebrafish embryo presents a similar picture, except that the zebrafish yolk plug is located ventral to the vegetal pole

(Kimmel et al., 1995). The rostral expression domains of *fgf8a* in the hindbrain primordia fuse in the midline because of convergence extension movements (Fig. 2A).

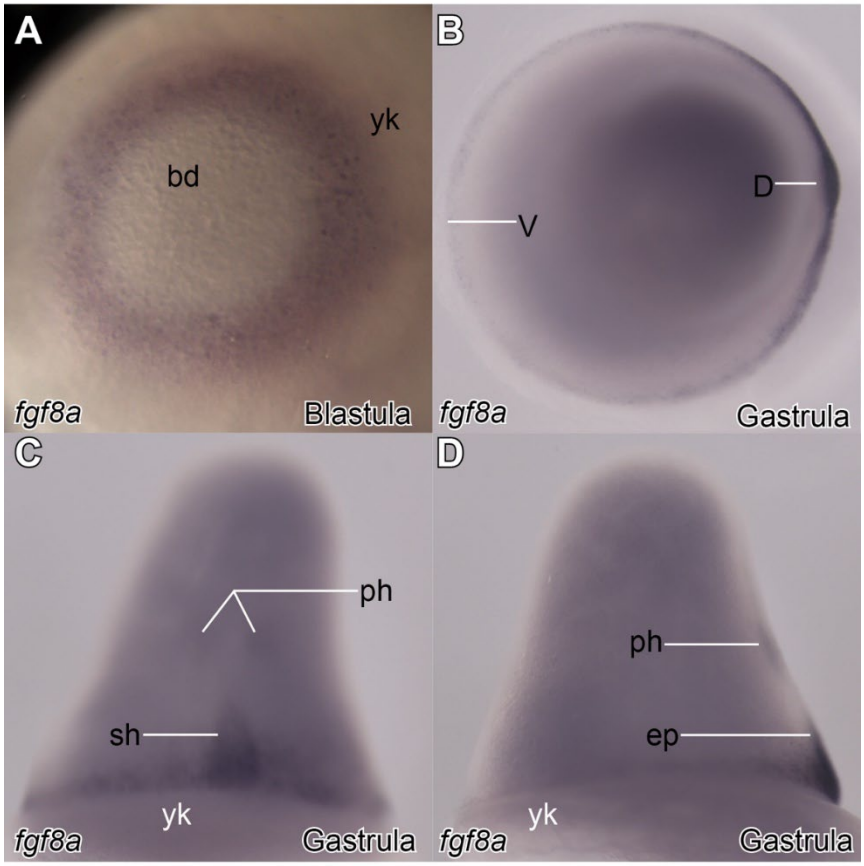

Figure 1 **Expression of *fgf8a* during the blastula and gastrula period of the rosy bitterling**. A, animal pole view, blastula stage, 6 hpf. B, C, and D, mid-gastrula stage, 15 hpf. B, animal pole view, dorsal at left. C, dorsal view, animal pole up. D, lateral view, animal pole up, dorsal at left. Key: bd, blastoderm; yk, yolk; D, dorsal; V, ventral; ph, presumptive hindbrain territory; sh, shield; ep, epiblast.

As blastokinesis advances, the embryo has migrated half-way up the yolk mass, being symmetrically doubled over either side of the animal pole; the blastopore is now closed (Fig. 2B, comparable in stage to Fig. 1E in Chang and Wu (1947)). The expression of *msx3* marks the boundary between the dorsal neural ectoderm, and the ventral non-neural ectoderm, and indicates the dorsal-ventral differentiation of the neural ectoderm. The rostral expression domains of *msx3* at the midbrain axial level are confluent in the midline, indicating the formation of the neural keel (Fig. 2C). The caudal expression pattern of *msx3* shows bilateral domains, indicating that the lateral neural plate has not yet converged in the midline at this axial level (Fig. 2D). In transverse sections (Fig. 3) it can be seen that the neuroectoderm has formed the neural plate in the midline. It has thickened in the dorsoventral axis to form the triangular neural keel at rostral axial levels (Fig. 3A) but remains as a flat neural plate caudally (Fig. 3B). The chordal mesoderm and somitic mesoderm undergo initial differentiation (Fig. 3B).

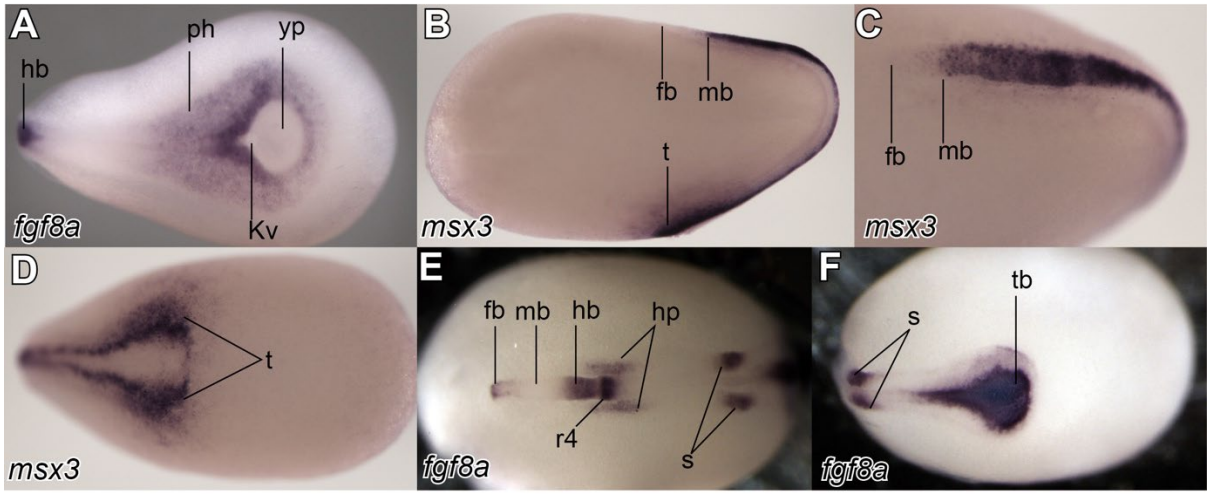

Figure 2 **Gene expression during the neurulation and somitogenesis periods of the rosy bitterling.** A, dorsal view, head to the left, 90% epiboly stage, 22.5 hpf. B, C and D, migration stage, 24.2 hpf; B is lateral view, dorsal up; C is dorsal view of head region, head to the left; D is dorsal view of the tail part, tail to the right. E and F, dorsal view of head and tail region respectively, head to the left, 3-somite stage, 25.5 hpf. Key: hb, hindbrain; ph, paraxial hypoblast; Kv, Kupffer's vesicle; yp, yolk plug; fb, forebrain; mb: midbrain; t, tail; r4, rhombomere 4; hp, heart primordia; s, somite; tb, tail bud. Stages according to Yi et al. (2021).

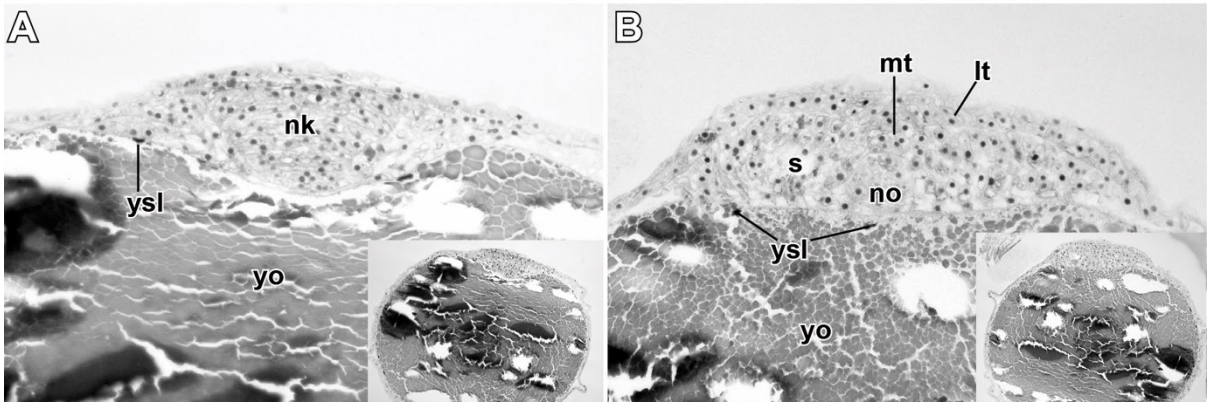

Figure 3 **Transverse sections through the dorsal side of a rosy bitterling embryo at the migration stage**. 24 hpf, H&E staining. The embryo lies symmetrically over either side of the animal pole. A and B are on opposite sides of the same section, dorsal up. A, the neural keel (nk) becomes visible at rostral axial levels. B, the neural plate at the caudal level, the median thickening (mt) of the neural plate immediately adjacent to the notochord (no), the lateral thickening (lt) overlay on somitic mesoderm (s). Key: ysl, nucleus of yolk syncytial layer; yo, yolk mass.

Body elongation during somitogenesis is the second phase of blastokinesis

With the progress of blastokinesis, the head of the embryo approaches the vegetal pole (Fig. 2E) and the tail approaches the animal pole (Fig. 2F). At the 3-somite stage *fgf8a* expression is seen in the forebrain, hindbrain, lateral plate mesoderm, somitic mesoderm and tailbud (Fig. 2E and F). Hybridization in the forebrain is particularly intense in the anterior neural ridge. The hindbrain expression extends from the presumptive MHB (midbrain-hindbrain boundary) to r4 (rhombomere 4), where it shows intense hybridization. Expression in the lateral plate mesoderm, bilaterally at the axial level of r4, indicates the induction of the cardiogenic fields. Segmental expression marks out the newly formed somites. The expression in the tailbud region is uniform, with no indication of a dorsal-ventral gradient in expression.

At the end of blastokinesis (the somite-6 stage), the YSEs project from the body in the ventral-dorsal direction; the yolk constriction on the ventral surface is prominent (Figure 4A, comparable to Fig. 1F in Chang and Wu (1947). At this stage, the expression of *fgf8a* is similar to the previous stage except that segmental expression in hindbrain becomes more obvious. There is now expression in r1, r2 and r4 but not in r3 (Fig. 4B). The expression of *fgf8a* in the differentiated somites becomes more restricted to the anterior somite border of somites 1-6. During the hatching period, at the 10-somite stage, the YSEs become more prominent (compare Figure 4B and D), and the rostral protrusion of the YE (yolk extension) appears. Hybridization of *fgf8a* in the hindbrain decreases, while the expression intensity at the MHB is still high. Hybridization to the anterior neural ridge of the forebrain domain appears stronger than the previous stage.

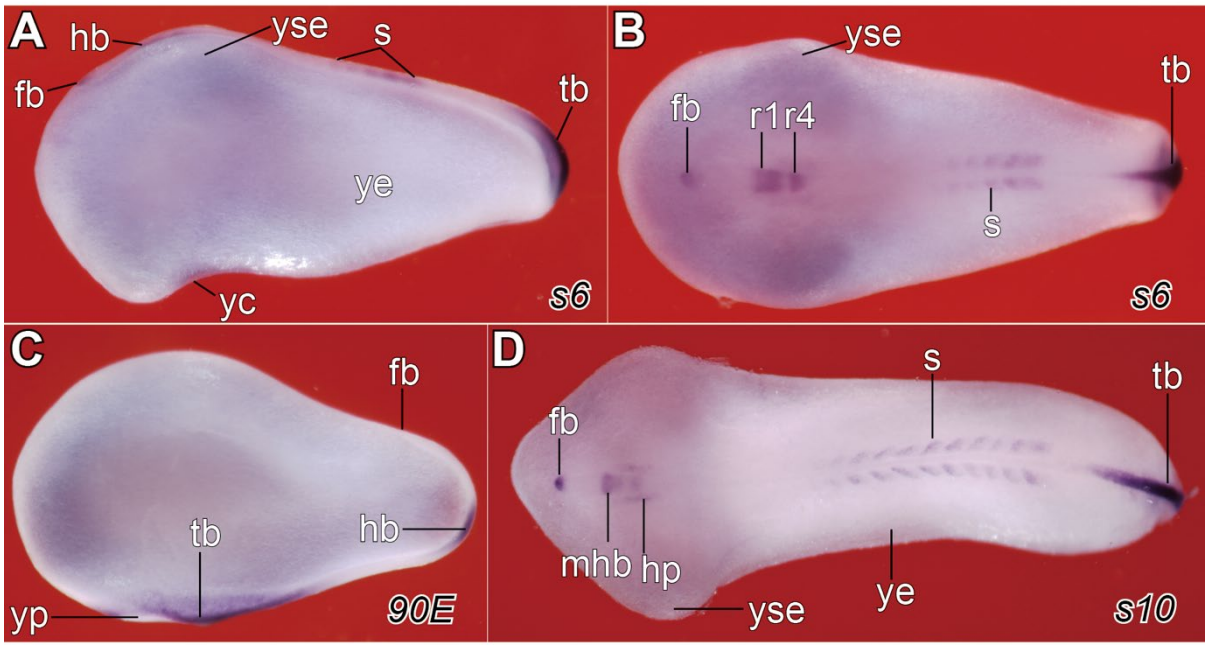

Figure 4 **Expression of *fgf8a* in the rosy bitterling embryo showing the elongation of embryo**. A and C, lateral aspect, head to the left. B and D, dorsal aspect, head to the left. A and B, 6-somite stage, 27 hpf. C, 90% epiboly stage, 22.5 hpf. D, 10-somite stage, 30 hpf. Comparing A and C, it can be seen that the hindbrain region is displaced from the animal pole towards the vegetal pole. Compare B and D for the elongation of the embryo trunk before and after hatching. Key: fb, forebrain; hb, hindbrain; tb, tail bud; r1, rhombomere 1; r4, rhombomere 4; yp, yolk plug; yc, yolk constriction; ye, yolk extension; yse, yolk sac extension; mhb: midbrain-hindbrain boundary; tb, tail bud; hp, heart primordium; s, somite.

Hatching of the embryo from the vegetal end of the chorion

Using time-lapse video recording of live embryos, we observed the hatching of embryos from the chorion. The process of hatching is very rapid, taking only 1 – 2 min. We hypothesize that the vegetal pole of the chorion is ruptured due to an increase in internal pressure, resulting in turn from the growing rostral protrusion of the YE (Fig. 5A to C). The expression of *krt8* in the bitterling embryo is restricted to the rostral protrusion of YE and YSEs before and after the hatching events at 29 hpf and 31 hpf (Fig. 5D to I). By contrast, *krt8* is expressed in the zebrafish embryo in the epidermis over the whole embryo up to 48 hpf (Fig. 5J to L). We suggest that the high local expression of *krt8* in the bitterling on the rostral protrusion of the YE and YSEs is related to cell aggregation and advanced keratinocyte differentiation. This in turn may facilitate the rupture of the chorion.

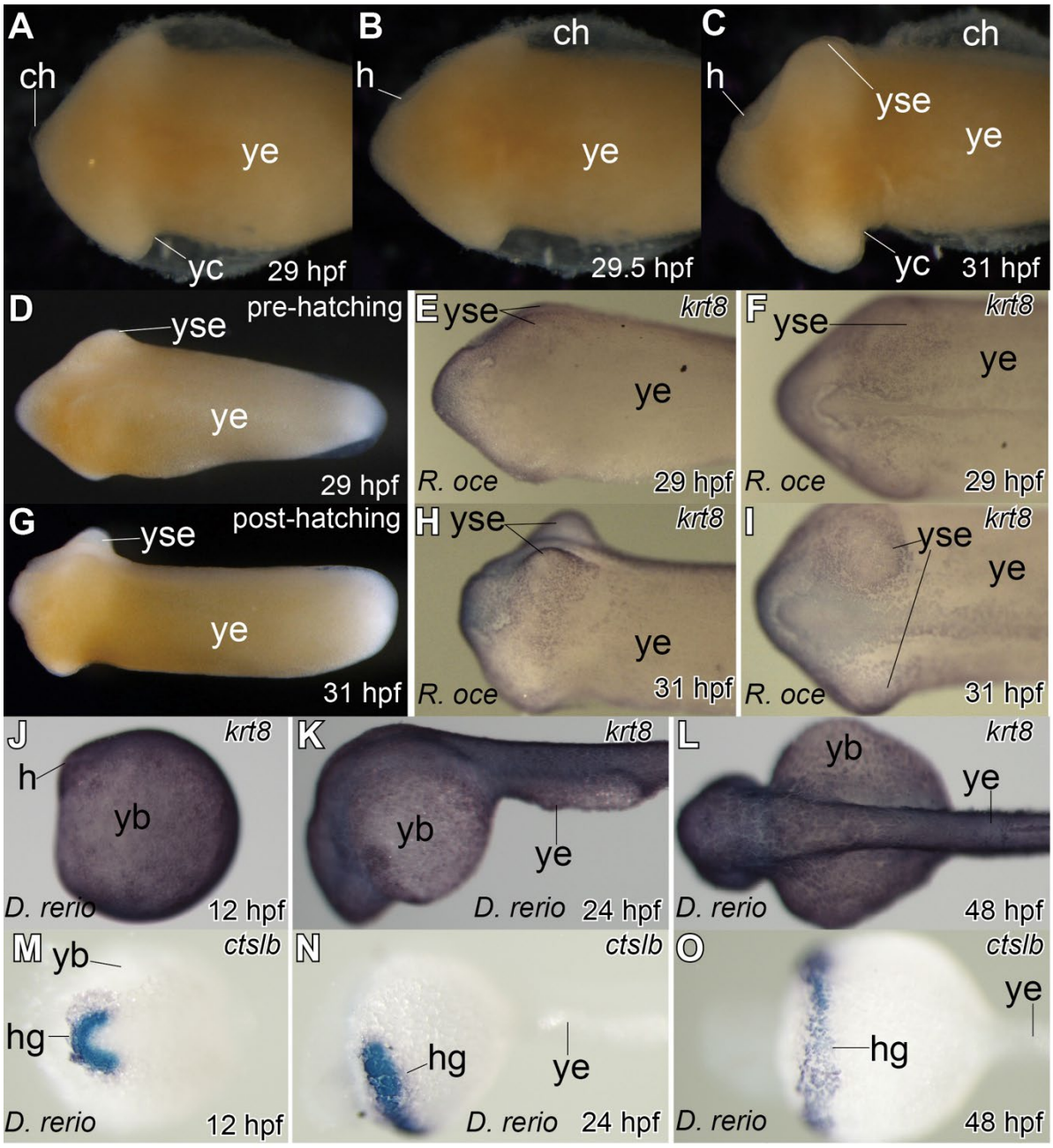

Figure 5 **Gene expression in the rosy bitterling during the hatching period**. All with head to the left. A to C, lateral view of bitterling embryos showing the hatching process. By 29 hpf, embryo before hatching with intact chorion (A); 30 min later, head and the anterior yolk extension protrudes from the chorion (B); by 31 hpf, the yolk sac extension (yse) and yolk constriction (yc) protrude from the chorion (C). D to I show *krt8* expression in *R. ocellatus* before and after hatching. Notice that the hybridization is particularly strong at the anterior yolk extension and the bilateral yolk sec extensions. J to L present the ubiquitous expression of *krt8* during zebrafish (*Danio rerio*) embryonic development. M to O present the specific expression of *ctslb* marking out the hatching gland cells of the zebrafish embryo. Key: ch, chorion; h, head; yc, yolk constriction; ye, yolk extension; yse, yolk sac extension; yb, yolk ball; hg, hatching gland.

We find no expression of *ctslb* in bitterling embryos during the hatching event (3-, 10- and 35-somite stages, data not shown). However, we find intense expression of *ctslb* in pre-hatching stages in the zebrafish (Fig. 5M to O). This result is consistent with our hypothesis that the hatching

of bitterlings is purely physical, with no involvement of a hatching-gland enzyme. Therefore, we conclude that the rupture site of the chorion is not random, but is consistently at the vegetal pole, in front of the rostral protrusion of the YE.

Blastokinesis determines the orientation of the post-hatching embryo in the host mussel

In the dissected host mussel, the main parasitic site of the bitterling embryo is the interlamellar space (Fig. 6A). This space is divided into parallel water tubes by the interlamellar junction (Fig. 6B). From our observations, the animal pole of the newly oviposited egg is always towards the opening of the water tube at the dorsal side of the host mussel (Fig. 6B). During blastokinesis, the orientation of embryo changes so that the head moves gradually to the vegetal pole (Fig. 6C). Consequently, when the embryo hatches out rostrally at the vegetal end, the newly hatched embryo is oriented towards the blind end of the water tube at the ventral side of the host mussel (Fig. 6E).

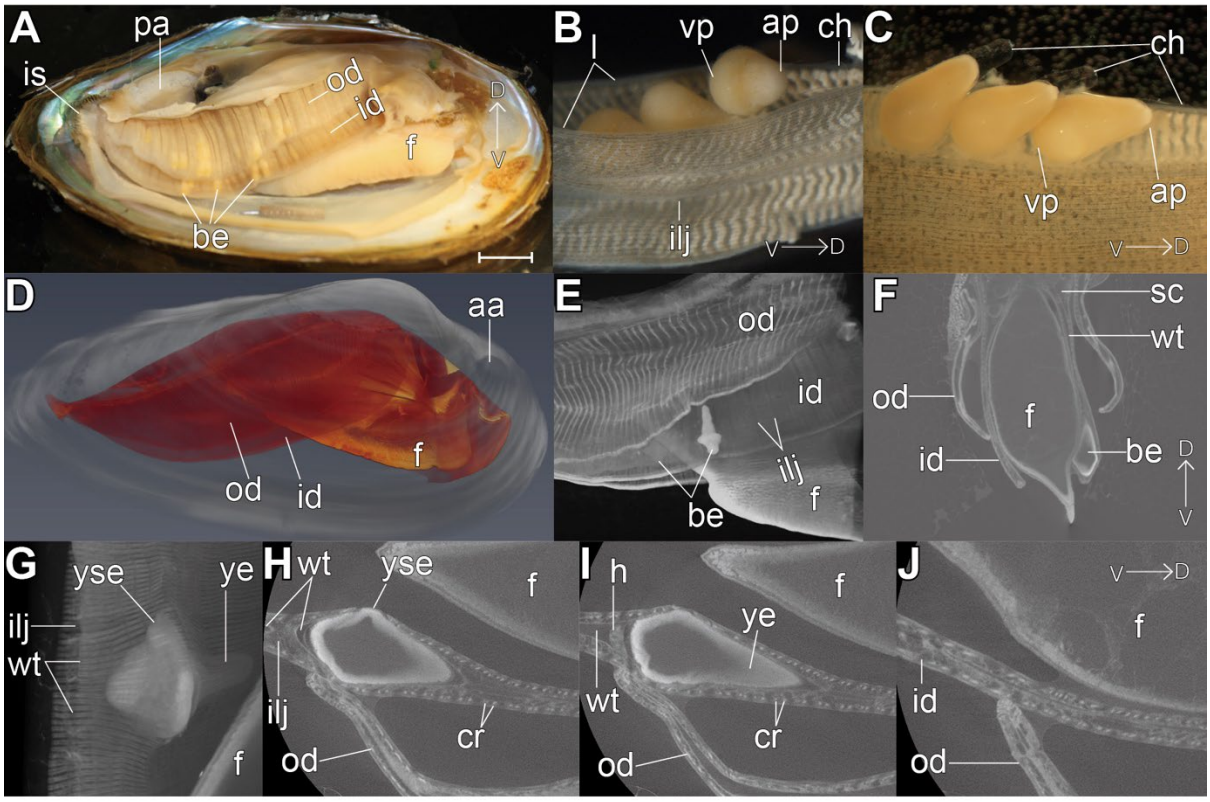

Figure 6 **Rosy Bitterling embryos in the interlamellar space of the host mussel (*Anodonta anatine*).** A shows a host mussel gravid with bitterling embryos, the right shell removed, dorsal up, anterior to the right. B and C are macro photographs of the gill lamellae occupied by bitterling embryos. Notice that the pre-hatching embryos are oriented with their animal pole dorsal to the gill lamellae. D, microCT reconstruction of an intact mussel. The internal soft tissue is pseudo-colored, dorsal up, anterior to the right. E to J is microCT scan results of a gravid host mussel. E and G, volume rendering view of mussel gills and bitterling embryos. F, transverse virtual section of the mussel gill lamellae, dorsal up. H to J, coronal virtual section of the bitterling embryo, head to the left. Keys: is, inhalant siphon; pa, posterior abductor muscle; aa, anterior abductor muscle; f, foot; be, bitterling embryo; od, outer demibranchs; id, inner demibranchs; wt, water tube; l, gill lamellae; ap, animal pole of bitterling embryo; vp, vegetal pole of bitterling embryo; ilj, interlamellar junction; h, head; ye, yolk extension; yse, yolk sac extension; sc, suprabranchial chamber; cr, chitinous rods. The dorsal-ventral body axis of the mussel is indicated by an arrow from V towards D. Scale bar in A is 10 mm.

Compared with a non-parasitized mussel (Fig. 6D), the gills of bitterling host-mussels have irregular folds and the interlamellar space is obviously dilated (Fig. 6E and F). At the site occupied by the bitterling embryo, 2-3 water tubes are merged to form a large chamber (Fig. 6G and J) because of the growth of YSEs. We also found damage to the interlamellar junction and broken lamellar filaments surrounding the enlarged YSEs (Fig. 6G). The gill filaments are closely attached to the yolk sac of the bitterling embryo, leaving no space for movements of the embryo before the YSEs disappears (Fig. 6H to J). Therefore, the bitterling post-hatching embryo is held in the gill water tube in this position for 3-4 weeks until the yolk mass has been totally consumed and the YSEs have disappeared.

Discussion

We have examined the unique blastokinesis process and early embryonic development of the bitterling *R. ocellatus* for the first time using molecular markers. Our data suggest that the blastokinesis in bitterlings is actually the convergent-extension movement during gastrulation and neurulation, followed by body elongation during somitogenesis. We also provide evidence that blastokinesis is functional, because it provides a secure body direction of post-hatching embryos in the water tube of the host mussel.

Now we can answer the question we posed in the introduction: what is the relationship between insect blastokinesis and bitterling blastokinesis? In short, these two types of blastokinesis are functionally different. In bitterlings, the distinct advantage of blastokinesis is related to the body direction during hatching, and does not function in agitating the yolk mass. We also show that, in the bitterling, the changes of embryo direction are like a 'front-flip' on the yolk mass, in contrast to the 'back flip' seen in insects (e.g., milkweed bug, *Oncopeltus fasciatus*; Panfilio, 2008). Therefore, it is difficult to find homology in regulatory genes. However, we suggest that blastokinesis may be related to the large quantity of yolk amount in bitterlings because it does not occur in *Drosophila melanogaster* (the fruit fly), the embryos of which have very reduced extraembryonic tissue (Panfilio, 2008; Saenko et al., 2008).

We have shown that yolk plug closure in the rosy bitterling and the zebrafish embryos takes place opposite the vegetal pole (dorsally *vs*. ventrally), indicating that the ventral blastoderm lip migrates faster than the dorsal lip in the bitterling. In zebrafish, the migration of the blastoderm is called epiboly (Délot et al., 1999; Fürthauer et al., 1997; Kimmel et al., 1995; Li et al., 2007; Xiong et al., 2014). We speculate that epiboly in the bitterling shows differences in migration rate compared to the zebrafish that may be related to the shape of the yolk. Our hypothesis is that the specialised shape and size of the bitterling yolk affects the diffusion of molecular signals that regulate the dorsal-ventral differentiation during convergence and extension. The body orientation during hatching is important in at least two respects.

First, if the opening of the chorion and the body orientation are random, then it may sometimes happen by chance that post-hatching embryos inside the water tube are aligned head-to-head. This orientation may be maladaptive if it leads to competetition between embryos of for oxygen and space. As we have shown in this study, all bitterling embryos hatch from the vegetal side of the chorion, opposite to the site of micropyle, and all are oriented in the same direction. We suggest that this arrangement allows all embryos to make the most effective use of the interlamellar space.

Second, the hatched embryos always have their heads directed towards the blind end of the gill filaments. In the eulamellibranch gill, the water runs into the partitioned water tubes through ostia. Inside each water tube, water moves dorsally and empties into the suprabranchial chamber, then out to the environment from the excurrent siphon (Medler and Silverman, 2001; Medler et al., 1999). It has been reported that mussels can eject premature bitterling embryos by a sudden burst of high velocity water flow (Mills and Reynolds, 2003; Reichard et al., 2007; Rouchet et al., 2017). With their heads facing the blind end, embryos can either resist ejection by being anchored to the gill filament via their wing-like YSEs (during the early developmental period) or can swim against the water current (when capable of movement).

The bitterling embryo provides an example how small modifications in yolk shape and egg size affect morphogenetic movements of the extraembryonic tissue (the yolk sac and YSEs) during gastrulation and somitogenesis. And these subtle shifts are amplified to produce an adaptive variation known as blastokinesis. This is in consistent with the concept of developmental penetrance of adaptations (Bickelmann et al., 2012; Richardson, 1999). This theory states that evolutionary adaptations appearing at later stages of development, can result from the modification of early stages of development.

References

Aldridge, D. C. (1999). Development of European bitterling in the gills of freshwater mussels. *J. Fish Biol.* **54**, 138–151.

Arai, R. (1988). *Acheilognathus melanogaster*, a senior synonym of *A. moriokae*, with a revision of the genera of the subfamily Acheilogathinae (Cypriniformes, Cyprinidae). *Bul Nat Sci Mus Tokyo Ser A* **14**, 199–213.

Awata, S., Sasaki, H., Goto, T., Koya, Y., Takeshima, H., Yamazaki, A. and Munehara, H. (2019). Host selection and ovipositor length in eight sympatric species of sculpins that deposit their eggs into tunicates or sponges. *Mar. Biol.* **166**, 59.

Bickelmann, C., Mitgutsch, C., Richardson, M. K., Jiménez, R., de Bakker, M. A. G., Sánchez-Villagra, M. R., Jimenez, R., de Bakker, M. A. G. and Sanchez-Villagra, M. R. (2012). Transcriptional heterochrony in talpid mole autopods. *Evodevo* **3**, 16.

Chang, H. W. (1948). Life history of the common Chinese bitterling, *Rhodeus ocellatus*. *Sinensia* **19**, 12–22.

Chang, H. W. and Wu, H. W. (1947). On the blastokinesis occurring in the egg of the common Chinese Bitterling, *Rhodeus ocellatus*. *Sinensia* **17**, 15–22.

Cheng, P., Yu, D., Liu, S., Tang, Q. and Liu, H. (2014). Molecular phylogeny and conservation priorities of the subfamily Acheilognathinae (Teleostei: Cyprinidae). *Zool. Sci* **31**, 300–308.

Délot, E., Kataoka, H., Goutel, C., Yan, Y.-L., Postlethwait, J., Wittbrodt, J. and Rosa, F. M. (1999). The BMP-related protein Radar: a maintenance factor for dorsal neuroectoderm cells? *Mech. Dev.* **85**, 15–25.

Dorey, K. and Amaya, E. (2010). FGF signalling: diverse roles during early vertebrate embryogenesis. *Development* **137**, 3731–3742.

Eisenhoffer, G. T., Slattum, G., Ruiz, O. E., Otsuna, H., Bryan, C. D., Lopez, J., Wagner, D. S., Bonkowsky, J. L., Chien, C. Bin, Dorsky, R. I., et al. (2017). A toolbox to study epidermal cell types in zebrafish. *J Cell Sci* **130**, 269–277.

Fürthauer, M., Thisse, C. and Thisse, B. (1997). A role for FGF-8 in the dorsoventral patterning of the zebrafish gastrula. *Development* **124**, 4253–64.

Imboden, M., Goblet, C., Korn, H. and Vriz, S. (1997). Cytokeratin 8 is a suitable epidermal marker during zebrafish development. *C R Acad Sci III* **320**, 689–700.

Kawamura, K., Ueda, T., Arai, R. and Smith, C. (2014). Phylogenetic relationships of bitterling fishes (Teleostei: Cypriniformes: Acheilognathinae), inferred from mitochondrial cytochrome B sequences. *Zool. Sci* **31**, 321–329.

Khlopova, A. V. and Kul'bachnyi, S. (2013). Histological structure of the female gonads and ovipositor of the European bitterling, *Rhodeus amarus* (Bloch, 1782) (Cyprinidae: Acheilognathinae). *Acta Zool.* **94**, 355–363.

Kim, Y. U. and Park, Y. S. (1985). Egg development and larvae of the rose bitterling *Rhodeus ocellatus* (KNER). *Korean J. Fish. Aquat. Sci.* **18**, 586–593.

Kimmel, C. B., Ballard, W. W., Kimmel, S. R., Ullmann, B. and Schilling, T. F. (1995). Stages of embryonic development of the zebrafish. *Dev. Dyn.* **203**, 253–310.
Kunz, Y. W. (2004). *Developmental Biology of Teleost Fishes*. Dordrecht: Springer Netherlands.
Leung, T. L. F. (2014). Fish as parasites: An insight into evolutionary convergence in adaptations for parasitism. *J. Zool.* **294**, 1–12.
Li, Z., Korzh, V. and Gong, Z. (2007). Localized rbp4 expression in the yolk syncytial layer plays a role in yolk cell extension and early liver development. *BMC Dev. Biol.* **7**, 117.
Medler, S. and Silverman, H. (2001). Muscular Alteration of Gill Geometry in vitro: Implications for Bivalve Pumping Processes. *Biol. Bull.* **200**, 77–86.
Medler, S., Thompson, C. C., Dietz, T. H. and Silverman, H. (1999). Ionic effects on intrinsic gill muscles in the freshwater bivalve, Dreissena polymorpha. *Comp. Biochem. Physiol. - A Mol. Integr. Physiol.* **122**, 163–172.
Mills, S. C. and Reynolds, J. D. (2003). The bitterling-mussel interaction as a test case for co-evolution. *J. Fish Biol.* **63**, 84–104.
Nagata, Y. and Miyabe, H. (1978). Development Stages of the Bitterling, *Rhodeus ocellatus ocellatus* (Cyprinidae). *Mem. Osaka Kyoiku Univ. III, Nat. Sci. Appl. Sci.* **26**, 171–181.
Needham, J. (1942). *Biochemistry and morphogenesis*. Cambridge: University Press.
Olt, A. (1893). Lebensweise und Entwicklung des Bitterlings. *Zeitschrift für wissenschaftliche Zool.* **55**, 543–575.
Panfilio, K. A. (2008). Extraembryonic development in insects and the acrobatics of blastokinesis. *Dev. Biol.* **313**, 471–491.
Panfilio, K. A. (2009). Late extraembryonic morphogenesis and its zenRNAi-induced failure in the milkweed bug Oncopeltus fasciatus. *Dev. Biol.* **333**, 297–311.
Phillips, B. T., Kwon, H. J., Melton, C., Houghtaling, P., Fritz, A. and Riley, B. B. (2006). Zebrafish msxB, msxC and msxE function together to refine the neural-nonneural border and regulate cranial placodes and neural crest development. *Dev. Biol.* **294**, 376–390.
Reichard, M., Liu, H. and Smith, C. (2007). The co-evolutionary relationship between bitterling fishes and freshwater mussels: insights from interspecific comparisons. *Evol. Ecol. Res.* **9**, 239–259.
Richardson, M. K. (1999). Vertebrate evolution: The developmental origins of adult variation. *BioEssays* **21**, 604–613.
Rouchet, R., Smith, C., Liu, H. Z., Methling, C., Douda, K., Yu, D., Tang, Q. Y. and Reichard, M. (2017). Avoidance of host resistance in the oviposition-site preferences of rose bitterling. *Evol. Ecol.* **31**, 769–783.
Saenko, S. V., French, V., Brakefield, P. M. and Beldade, P. (2008). Conserved developmental processes and the formation of evolutionary novelties: examples from butterfly wings. *Philos Trans R Soc L. B Biol Sci* **363**, 1549–1555.
Smith, C. (2016). Bayesian inference supports the host selection hypothesis in explaining adaptive host specificity by European bitterling. *Oecologia* **183**, 1–11.
Smith, C., Reichard, M., Jurajda, P. and Przybylski, M. (2004). The reproductive ecology of the European bitterling (*Rhodeus sericeus*). *J. Zool.* **262**, 107–124.
Smith, C., Warren, M., Rouchet, R. and Reichard, M. (2014). The function of multiple ejaculations in bitterling. *J. Evol. Biol.* **27**, 1819–1829.
Spence, R. and Smith, C. (2013). Rose bitterling (Rhodeus ocellatus) embryos parasitize freshwater mussels by competing for nutrients and oxygen. *Acta Zool.* **94**, 113–118.
Suzuki, N. (2006). Egg and larval development of the bitterling, *Rhodeus pseudosericeus* (Cyprinidae). *Japanese J. Ichthyol.* **53**, 47–54.
Tada, M. and Heisenberg, C.-P. (2012). Convergent extension: using collective cell migration and cell intercalation to shape embryos. *Development* **139**, 3897–3904.
Virta, V. C. and Cooper, M. S. (2009). Ontogeny and phylogeny of the yolk extension in embryonic cypriniform fishes. *J. Exp. Zool. Part B Mol. Dev. Evol.* **312**, 196–223.
Vogel, A. M. and Gerster, T. (1997). Expression of a zebrafish Cathepsin L gene in anterior mesendoderm and hatching gland. *Dev. Genes Evol.* **206**, 477–479.
Williams, M. L. K. and Solnica-Krezel, L. (2020). Cellular and molecular mechanisms of convergence and extension in zebrafish. In *Current Topics in Developmental Biology*, pp. 377–407. Academic Press Inc.
Xiong, F., Ma, W., Hiscock, T. W., Mosaliganti, K. R., Tentner, A. R., Brakke, K. A., Rannou, N., Gelas, A., Souhait, L., Swinburne, I. A., et al. (2014). Interplay of Cell Shape and Division Orientation Promotes Robust Morphogenesis of Developing Epithelia. *Cell* **159**, 415–427.